

siRNA-mediated gene silencing: a global genome view

Dimitri Semizarov*, Paul Kroeger and Stephen Fesik

Global Pharmaceutical Research and Development, Abbott Laboratories, 100 Abbott Park Road, Abbott Park, IL 60064, USA

Received March 23, 2004; Revised June 4, 2004; Accepted July 1, 2004

ABSTRACT

The task of specific gene knockdown *in vitro* has been facilitated through the use of short interfering RNA (siRNA), which is now widely used for studying gene function, as well as for identifying and validating new drug targets. We explored the possibility of using siRNA for dissecting cellular pathways by siRNA-mediated gene silencing followed by gene expression profiling and systematic pathway analysis. We used siRNA to eliminate the *Rb1* gene in human cells and determined the effects of *Rb1* knockdown on the cell by using microarray-based gene expression profiling coupled with quantitative pathway analysis using the GenMapp and MappFinder software. Retinoblastoma protein is one of the key cell cycle regulators, which exerts its function through its interactions with E2F transcription factors. *Rb1* knockdown affected G₁/S and G₂/M transitions of the cell cycle, DNA replication and repair, mitosis, and apoptosis, indicating that siRNA-mediated transient elimination of Rb1 mimics the control of cell cycle through Rb1 dissociation from E2F. Additionally, we observed significant effects on the processes of DNA damage response and epigenetic regulation of gene expression. Analysis of transcription factor binding sites was utilized to distinguish between putative direct targets and genes induced through other mechanisms. Our approach, which combines the use of siRNA-mediated gene silencing, mediated microarray screening and quantitative pathway analysis, can be used in functional genomics to elucidate the role of the target gene in intracellular pathways. The approach also holds significant promise for compound selection in drug discovery.

INTRODUCTION

The process of RNA interference is mediated by double-stranded RNA, which is cleaved by the enzyme DICER into duplexes 21–23 nt in length containing a 2 nt overhang at the 3' end of each strand (1). The task of specific gene knockdown *in vitro* has been facilitated through the use of short interfering RNA (siRNA) (2). The use of RNA interference (RNAi) for inhibiting gene expression represents a powerful tool for exploring gene function, identifying and

validating new drug targets, and treating disease (3–8). siRNA may also prove to be a useful tool for dissecting cellular pathways, if siRNA-mediated gene knockdown is followed by a systematic analysis of downstream effects.

Here, we combined the use of siRNA, microarray technologies and quantitative pathway analysis to determine the effects of a gene knockdown on the cell. The combination of the siRNA and microarray technologies is a powerful tool in large-scale genomics experiments, particularly if the vast amount of gene expression data is systematically analyzed in the context of the biological pathways. We have previously used DNA microarrays to assess the consequences of gene silencing on a genome-wide scale (9). In this work, we used siRNA to silence the retinoblastoma gene (*Rb1*) in human cells and comprehensively analyzed the resulting transcriptional activation pattern using the Gene Ontology (GO) pathway classification (10).

The *Rb1* gene was chosen because of its critical role in cell cycle progression (11–13) and the dependence of its function on interactions with members of the E2F family of transcription factors. During the G₁ phase, Rb1 binds to and inactivates E2F-1, thus causing transcriptional repression of E2F-1 controlled genes. In the late G₁ phase, the Rb1 protein is phosphorylated by cyclin-dependent kinases 4 and 6 (CDK 4/6), which results in the dissociation of the Rb1/E2F-1 complex and subsequent activation of transcription of E2F-1 target genes (13–15). Previously identified E2F-1-controlled genes in rodents are involved in DNA biosynthesis and control of cell cycle progression (16–19), which is consistent with the role of *Rb1* in controlling the G₁/S cell cycle transition.

A systematic pathway analysis of the gene expression signatures associated with the knockdown of the target gene revealed a pattern generally consistent with those observed earlier upon E2F overexpression (16–19) and identified a number of genes involved in the CDK4/6–pRb–E2F pathway. An analysis of E2F binding sites has been performed for the genes induced upon *Rb1* knockdown to identify putative targets of the pathway. The proposed methodology may be used for systematic examination of intracellular pathways and selection of small molecule inhibitors in drug discovery.

MATERIALS AND METHODS

Cell culture and siRNA

Human non-small cell lung carcinoma cells H1299 were cultured in RPMI-1640 medium (Invitrogen Corp, Carlsbad, CA) supplemented with 10% fetal bovine serum (FBS)

*To whom correspondence should be addressed. Tel: +1 847 936 0299; Fax: +1 847 935 5165; Email: Dimitri.Semizarov@abbott.com

siRNA ID	Sequence
1	5'-GAUACCAGAUAUGUCAGAdTdT-3' (sense) 3'-dTdTTCUAUGGUCUAGUACAGUCU-5' (antisense)
2	5'-GUUGAAUUGCUAUGUCAAdTdT-3' 3'-dTdTCAACUAAUACGAUACAGUU-5'
3	5'-CCAGCAGUUCGAUAUCUAdTdT-3' 3'-dTdTGGGUCGUCAAGCUAUAGAU-5'
4	5'-ACUCUACCUCCCAUGUUGdTdT-3' 3'-dTdTUGAGAGUGGAGGGUACAAC
5	5'-CACCCAGGCGAGGUCAGAAAdTdT-3' 3'-dTdTGUUGGUCGCCUCCAGUCUU-5'
C	5'-GGGCGUCGAUCCUAAACCGdTdT-3' 3'-dTdTCCCGCAGCUAGGAUUGGCC-5'

Figure 1. siRNA sequences used in this work.

(Invitrogen). To maximize the specificity of targeting, siRNAs were designed using a previously described algorithm (9). The sense strand was included in the homology minimization algorithm together with the antisense strand, as it may influence the specificity of gene silencing (20,21). The sequences of the siRNAs used in this work are listed in Figure 1. Transfections were performed using the TransIT-TKO reagent (Mirus Corp., Madison, WI) according to the manufacturer's instructions. Cells were plated into 60 mm dishes (Corning) 24 h prior to transfections. At the time of transfection, the cell density was 5×10^5 cells/ml. Briefly, 3 μ l of 20 μ M siRNA solution and 15 μ l of the transfection reagent were incubated in 0.5 ml of serum-free RPMI-1640 media for 20 min to facilitate complex formation. The resulting mixture was added to the cells cultured in 2.5 ml of RPMI-1640. Each siRNA was transfected into two dishes of H1299 cells. The cells were lysed after 12 h to isolate total RNA.

Microarray profiling and pathway analysis

Total RNA was extracted using the Trizol reagent (Invitrogen) and purified on RNeasy columns (Qiagen). The quality of total RNA was monitored by using a BioAnalyzer (Agilent Technologies). Labeled cRNA was prepared according to the standard Affymetrix protocol using 5–10 μ g of total RNA as starting material. The labeled cRNA was hybridized to Human Genome U95Av2 chips (Affymetrix, Inc., Santa Clara, CA) containing $\sim 12,000$ genes and expressed sequence tags (ESTs). Microarray data were analyzed using ResolverTM software (Rosetta Inpharmatics, Kirkland, WA) and exported into Excel for pathway analysis.

For pathway analysis of the *Rb1* knockdown signature, we used the GeneMapp and MappFinder software packages (www.GenMapp.org) (22,23). The GeneMapp program contains dozens of pre-loaded pathway maps, which can be associated with an imported gene expression signature. To establish the associations between the *Rb1* knockdown signature and the affected pathways, the MappFinder program was used, which links gene expression data to the Gene Ontology hierarchy (10). The GO hierarchy provides a structure for organizing genes into biologically relevant subcategories, with a parent-child relationship between its terms. The subcategories can serve as a basis for identifying those processes showing correlated gene expression changes in an experiment. MappFinder calculates the percentage of the genes measured that meet a user-defined criterion (≥ 1.5 -fold change and P -value ≤ 0.05 in our analysis). This is done for each GO

node and for the cumulative total of the number of genes in a parent GO term combined with all its children. Using this percentage, as well as the Z-score, the GO terms can be ranked by the relative amount of gene expression changes. The three highest-level branches in the GO tree are biological processes, cellular components and molecular functions. Our analysis was limited to the biological processes branch.

Analysis of promoter regions for putative E2F binding sites

To identify putative E2F regulatory sites in the promoter region of *Rb1*-regulated genes, we retrieved, in batch mode, the presumed promoter region (–1000 to +200 bp) for as many genes as possible using the Promoser server at <http://biowulf.bu.edu/zlab/promoser/>. Of the 469 genes that were positively regulated by siRNAs targeted to *Rb1*, we were able to retrieve 398 upstream regions using the following parameters: quality metric of at least 1 and supporting sequences of at least 2. Accuracy of the sequence retrieval was then assessed by BLAST analysis of the sequences against the GenCarta (CompuGen) human sequence database. Additionally, the sequences were checked individually against the proposed region of transcription initiation defined in the DataBase of Transcriptional Start Sites (DBTSS) constructed by the University of Tokyo (<http://dbtss.hgc.jp/>). When there was ambiguity in the putative transcription start site (TSS), such as multiple distinct sites, the sequence was removed from consideration. Even though many genes have some degree of alternative transcription initiation, it was encouraging that for $\sim 90\%$ of the Promoser recovered sequences there was good agreement (generally within ± 100 bases) with the alignment of reference (e.g. NM_XXXXXX) and EST sequences in the DBTSS.

E2F transcription factor binding sites flanking the proposed transcription start site for each gene were predicted based on the rules determined previously by Kel *et al.* (24). Promoter sequences were analyzed using the E2F search site program (<http://compel.bionet.nsc.ru/FunSite.html>) established by Kel *et al.* with the following settings: weight matrix threshold of 0.8 and forbidden nucleotides at conserved positions not allowed. This approach was a compromise to permit the identification of as many sites as possible. We scanned nearly 500,000 bases of promoter sequence and found 1212 putative E2F sites. The average number of predicted E2F sites across all 398 up-regulated genes was 3.55 (range of 1–14) with an average Q -score of 0.87.

As shown previously by Kel *et al.* (24), we observed a distribution of E2F sites across our promoter regions that peaked at the start of transcription. To reduce false positives and maximize total positives, we filtered the data for E2F sites that had a Q -score of at least 0.86 and fell within –400 and +100 bases of the proposed start of transcription for each gene (24). This resulted in 238 sites distributed among 162 genes that represent high probability active E2F binding sites. As a check on our method, we examined genes from our list that were known to have E2F sites and found that many (e.g. *cdc6*, *cdc2*, *mcm2–mcm7*) were confirmed. Our analysis has identified a number of additional targets of the E2F-*Rb1* pathway possessing E2F sites. Among them are many genes associated with DNA replication/repair and related cellular processes. For example, our analysis has confirmed and extended the

observations of others (25) that the mini chromosome maintenance (MCM2–MCM7) family of proteins, involved in DNA replication and mitosis are regulated by E2F. All of the 6 MCM genes on the microarray contain at least one high probability site within 220 bases of the TSS and these sites have an average Q -score of 0.98.

RESULTS AND DISCUSSION

Gene expression signatures generated by siRNAs against *Rb1*

Initially, a total of eight siRNAs against *Rb1* were designed using a previously described algorithm (9). Prior to the microarray experiments, all 8 siRNAs were transfected into H1299 cells and tested for mRNA and protein knockdown at 12 h by quantitative RT–PCR and western blot, respectively. Five out of the eight siRNAs were found to efficiently eliminate the target mRNA and protein (Figure 2). These five duplexes, as well as a control random-sequence siRNA were used in subsequent experiments. The gene expression changes were evaluated relative to the control siRNA-treated cells. The control siRNA was chosen based on the minimal potential for cross-hybridization to sequences represented in the RefSeq database, as indicated by BLAST results. The control random-sequence siRNA caused few gene expression changes versus untreated cells; none of the genes from the *Rb1* knockdown signature was regulated by the control siRNA at the P -value cut-off of 0.05 (Supplementary Table 1). Since our goal was to examine the effects of *Rb1* knockdown, we wanted to make sure that only the specific on-target effects of the *Rb1* siRNA are analyzed. Therefore, we generated gene expression signatures for all five efficacious siRNAs (Supplementary Table 2) and then analyzed the common gene set. The use of multiple siRNAs is highly desirable as it allows one to eliminate potential non-specific effects unique to individual siRNAs. To increase the robustness of the microarray data analysis, biological duplicates were used for each siRNA, which brought the number of independent transfection experiments to 10. Human H1299 cells were transfected with the siRNAs and then lysed after 12 h. The 12 h time point was

chosen based on our previous gene expression studies with *Rb1* (data not shown) and earlier microarray studies of E2F-1 overexpression (18).

In our analysis of the data from the 10 *Rb1* knockdown experiments, we took a conservative approach and defined the *Rb1* knockdown signature as the overlap of the gene sets regulated by the individual *Rb1* siRNAs at the confidence level of 95%. First, we exported into Excel all the genes regulated in at least 1 experiment with a P -value ≤ 0.05 and a fold change of ≥ 1.5 . A combined redundant list of genes was then created for all 10 experiments. Only genes regulated by at least three siRNAs were retained for pathway analysis with MappFinder.

Pathway analysis of the *Rb1* knockdown signature

To systematically examine the effects of the *Rb1* knockdown on cellular processes, we used the GeneMapp and MappFinder software packages as described in Materials and Methods. Figure 3 presents the GO branches most significantly affected by *Rb1* knockdown. It can be seen that within the Cell Growth and Maintenance node, the most affected processes are in the Cell Cycle branch. This is consistent with the role of *Rb1* in the control of cell cycle and previously reported data on gene regulation by E2Fs (16–19,26). Among the child nodes within the Cell Cycle branch, the Mitotic Cell Cycle, DNA replication and Chromosome Maintenance, and Regulation of Cell Cycle processes are significantly associated with the elimination of the *Rb1* protein (Z -scores > 2). It has been previously reported that overexpression of E2Fs induces genes involved in the G_1/S transition, DNA replication and mitosis (16–19). Our observations are consistent with these data and thus indicate that elimination of *Rb1* by siRNA-mediated silencing releases E2Fs and induces E2F-mediated transcription.

Interestingly, although the *Rb1*/E2F mechanism is primarily known for its role in G_1/S regulation, the M phase and mitosis-related nodes were among the most affected in our analysis. Ishida *et al.* (17) have observed induction of some mitotic genes upon overexpression of E2Fs in mouse fibroblasts. The authors also showed that the induction of these genes is not simply a consequence of induced cell cycle progression. However to prove this hypothesis, it is important to establish

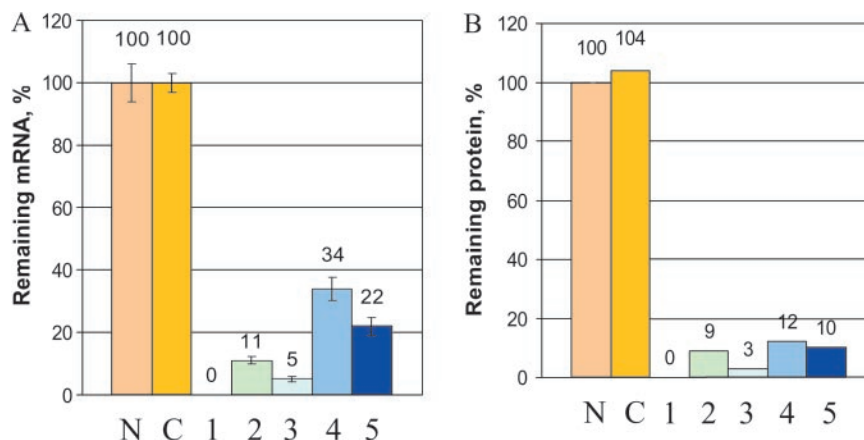


Figure 2. Elimination of the target mRNA (a) and protein (b) by siRNAs 1–5 against *Rb1*. In control assays, no siRNA was used (N) or a random-sequence control siRNA was used (C).

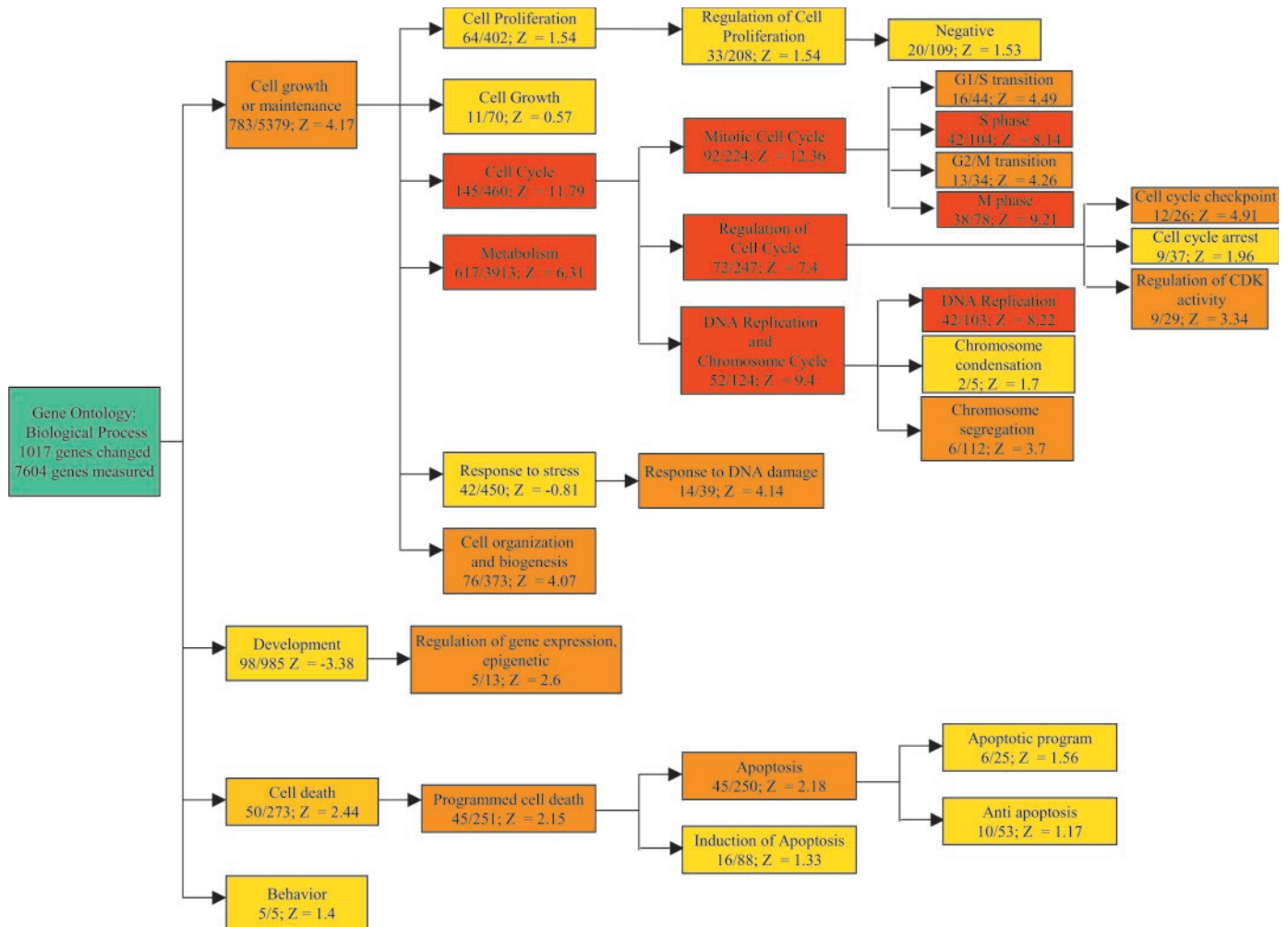


Figure 3. The pathway associations of the Rb knockdown signature. The Gene Ontology nodes strongly affected by the *Rb1* silencing are shown, along with the number of genes affected, number of genes present on the chip (in the *affected/present* format), and the Z-score, which indicates the relatedness of the gene expression signature to the process. The color of the box reflects the Z-score for the node (red, $Z \geq 5$; orange, $2 \leq Z \leq 5$; yellow, $Z \leq 2$).

these genes as direct targets of the CDK4/6–pRb–E2F pathway. This problem can be approached by identifying E2F-binding sites in the promoter regions of these genes (next subsection of Results and Table 1).

It can also be seen in Figure 3 that silencing of the *Rb1* gene induces apoptotic pathways, as evidenced by the Z-scores for the Programmed Cell Death/Apoptosis branch of the GO. This observation is consistent with the finding that overexpression of E2Fs leads to apoptosis (13,27). Thus, elimination of the Rb1 protein and analysis of the transcriptional consequences allowed us to observe the global pattern associated with a cell cycle transition and apoptosis. Elimination of the Rb1 protein by siRNA thus mimics the process of Rb1 phosphorylation and E2F release that occurs at the G₁/S transition.

Our analysis also reveals some potential novel pathway effects. For example, the Response to DNA damage node is significantly affected (Z-scores of 4.14), mostly due to the regulation of Chk1, ATM, ABL and BRCA1. It has been previously shown that overexpression of E2Fs induces genes, whose products execute DNA repair, such as MSH2, MSH6 and UNG (18). The most obvious explanation for this

induction was that it was related to initiation of DNA replication. Indeed, DNA repair function is complementary to DNA replication, as the latter process is not error-free and produces mismatches that need to be repaired. However, here we report that elimination of Rb1 affects the upstream regulators of the DNA damage pathway, such as ATM, Chk1 and ABL. These data suggest that *Rb1* is involved in the control of the DNA damage response in addition to the regulation of DNA replication and concurrent DNA repair. This is consistent with several earlier reports. In particular, it has been reported that DNA-damaging agents cause an increase in the E2F protein expression and its DNA binding capacity (28–30). Ren *et al.* (31) have suggested a role for E2Fs in checkpoint control based on results from a novel promoter binding assay. It has been suggested that both *pRb* and *p53* may play a role in DNA damage-induced G₁ arrest (31,32).

Another node affected by Rb1 knockdown is the Epigenetic Regulation of Gene Expression node. The Z-score of 2.6 reflects the regulation of 5 out of 13 genes in the node; specifically, DNA (cytosine-5)-methyltransferase 1 (NM_001379) was up-regulated 1.7-fold and STK-1 was

Table 1. Selected genes induced upon Rb knockdown

Gene description	Primary name	Accession no.	Mean FC	SD	Reference					E2F site
					(19)	(16)	(17)	(18)	(26)	
Cell cycle										
Serum-inducible kinase	SNK	AF059617	2.11	0.24						
Cyclin B2	CCNB2	AL080146	3.66	0.22			Yes		Yes	
Ras association (RalGDS/AF-6) domain family 1	RASSF1	AF061836	2.18	0.31						
Cyclin-dependent kinase inhibitor 2C (p18)	CDKN2C	AF041248	2.06	0.17			Yes		Yes	+
CDC28 protein kinase 2	CKS2	X54942	4.25	0.42						+
Cyclin F	CCNF	Z36714	3.43	0.13						
Minichromosome maintenance deficient 4	MCM4	X74794	7.38	2.09	Yes				Yes	+
Minichromosome maintenance deficient 2	MCM2	D21063	2.19	0.13				Yes	Yes	+
Transcription factor Dp-1	TFDP1	L23959	10.69	2.31	Yes	Yes			Yes	+
<i>Homo sapiens</i> DNA sequence from PAC 15005	E2F2	AL021154	2.46	0.10						+
CHK1 (checkpoint, <i>Schizosaccharomyces pombe</i>) homolog	CHEK1	AF016582	2.61	0.10						+
Cyclin A2	CCNA2	X51688	5.99	0.16			Yes			
Cyclin A1	CCNA1	U66838	5.61	0.50						
Cell division cycle 2, G ₁ to S and G ₂ to M	CDC2	Y00272	4.16	0.61			Yes	Yes		+
Cyclin E2	CCNE2	AF091433	5.27	0.81			Yes	Yes		+
Cyclin-dependent kinase inhibitor 3	CDKN3	L25876	4.61	0.43						
Activator of S phase kinase	ASK	AB028069	3.03	0.30						+
G ₁ to S phase transition 1	GSPT1	X17644	1.84	0.11						+
Cyclin C	CCNC	M74091	1.87	0.18						
Cyclin D3	CCND3	M92287	1.63	0.10						
Baculoviral IAP repeat-containing 5 (survivin)	BIRC5	U75285	2.79	0.49						
Serine/threonine kinase 15	STK15	AF011468	5.17	0.40						+
Cyclin B1	CCNB1	M25753	5.30	0.17			Yes		Yes	+
Polo (<i>Drosophila</i>)-like kinase	PLK	U01038	4.12	0.64					Yes	
Minichromosome maintenance deficient 3	MCM3	D38073	3.95	0.29			Yes			+
CDC20 (<i>Saccharomyces cerevisiae</i> , homolog)	CDC20	U05340	4.55	0.49					Yes	+
TTK protein kinase	TTK	M86699	3.63	0.44						+
Serine/threonine kinase 12	STK12	AF015254	3.12	0.22						
Serine/threonine kinase 18	STK18	Y13115	2.60	0.14					Yes	+
Budding uninhibited by benzimidazoles 1	BUB1	AF053305	5.02	0.46			Yes		Yes	
Pituitary tumor-transforming 1	PTTG1	AA203476	4.19	0.35			Yes			
Cell division cycle 25C	CDC25C	M34065	2.32	0.28						
Cyclin-dependent kinase 2	CDK2	M68520	1.58	0.04			Yes		Yes	
CDC28 protein kinase 1	CKS1	AA926959	1.64	0.08						
BTG family, member 3	BTG3	D64110	1.67	0.08	Yes	Yes				+
Putative lymphocyte G ₀ /G ₁ switch gene	G0S2	M69199	1.78	0.07						
DNA biosynthesis										
Methylenetetrahydrofolate dehydrogenase	MTHFD1	J04031	1.79	0.07						+
Ribonucleotide reductase M2 polypeptide	RRM2	X59618	21.37	6.37	Yes	Yes	Yes		Yes	+
CDC6 (cell division cycle 6, <i>S.cerevisiae</i>) homolog	CDC6	U77949	9.25	1.90						+
CDC45 (cell division cycle 45 homolog)-like	CDC45L	AJ223728	5.36	0.63						+
Polymerase (DNA directed), epsilon 2	POLE2	AF025840	4.37	0.41						+
Thymidine kinase 1, soluble	TK1	M15205	5.07	0.52			Yes			
Proliferating cell nuclear antigen	PCNA	M15796	4.59	0.20	Yes		Yes	Yes	Yes	
Thymidylate synthetase	TYMS	X02308	5.17	0.53			Yes	Yes		
Ribonuclease HL, large subunit	RNASEHI	Z97029	3.31	0.39						
Thymidine kinase 1, soluble	TK1	K02581	3.27	0.14						
Replication protein A3 (14 kDa)	RPA3	L07493	3.18	0.17				Yes		+
Topoisomerase (DNA) II alpha (170 kDa)	TOP2A	AI375913	3.02	0.27			Yes	Yes	Yes	
Ribonucleotide reductase M1 polypeptide	RRM1	X59543	2.84	0.16	Yes		Yes		Yes	
<i>H.sapiens</i> clone 24767 mRNA		AF070552	2.65	0.20						+
Vaccinia related kinase 1	VRK1	AB000449	2.72	0.24	Yes					+
Minichromosome maintenance deficient 5	MCM5	X74795	2.56	0.12					Yes	+
Deoxythymidylate kinase (thymidylate kinase)	DTYMK	L16991	2.52	0.22						+
Replication factor C (activator 1) 5 (36.5 kDa)	RFC5	L07540	2.43	0.18						+
Topoisomerase (DNA) II alpha (170 kDa)	TOP2A	J04088	2.60	0.12			Yes	Yes		
Polymerase (DNA directed), gamma	POLG	W74442	2.43	0.32						+
Primase, polypeptide 2A (58 kDa)	PRIM2A	X74331	2.25	0.45			Yes	Yes	Yes	+
Primase, polypeptide 1 (49 kDa)	PRIM1	X74330	2.22	0.13			Yes			+
Replication factor C (activator 1) 3 (38 kDa)	RFC3	L07541	2.07	0.14	Yes		Yes			+
Phosphoribosyl pyrophosphate synthetase 2	PRPS2	Y00971	1.97	0.12						
Replication factor C (activator 1) 2 (40 kDa)	RFC2	NM_002914	2.03	0.11						
Chromatin assembly factor 1, subunit A (p150)	CHAF1A	U20979	1.89	0.11	Yes					+
Replication factor C (activator 1) 4 (37 kDa)	RFC4	M87339	1.87	0.17	Yes			Yes		
Guanine monophosphate synthetase	GMPS	U10860	2.36	0.23						+
Topoisomerase (DNA) II binding protein	TOPBP1	D87448	1.85	0.16						+
Non-metastatic cells 1, protein (NM23A)	NME1	X17620	1.86	0.06						

Table 1. Continued

Gene description	Primary name	Accession no.	Mean FC	SD	Reference					E2F site
					(19)	(16)	(17)	(18)	(26)	
CTP synthase	CTPS	X52142	1.65	0.07						
Phosphoribosyl pyrophosphate synthetase 1	PRPS1	D00860	1.68	0.09						
Replication protein A1 (70 kDa)	RPA1	M63488	1.66	0.09		Yes				+
Replication factor C (activator 1) 4 (37 kDa)	RFC4	M87339	1.64	0.09	Yes					
Uridine monophosphate kinase	UMPK	D78335	1.66	0.10						
Uridine monophosphate synthetase	UMPS	J03626	1.62	0.07						
Minichromosome maintenance deficient 6	MCM6	D84557	1.72	0.12				Yes	Yes	+
Nucleoside phosphorylase	NP	X00737	1.61	0.11						
Adenosine kinase	ADK	U50196	1.66	0.16						+
Minichromosome maintenance deficient 7	MCM7	D55716	1.60	0.08	Yes		Yes		Yes	+
Cell line HL-60 alpha topoisomerase	904_s_at	L47276	2.95	0.21			Yes	Yes		
Putative dimethyladenosine transferase	HSA9761	AF091078	1.79	0.08						
Putative dimethyladenosine transferase	HSA9761	AF091078	1.81	0.20						
Origin recognition complex, subunit 3-like	ORC3L	AL080116	1.69	0.12						+
Chromosome 11, BAC CIT-HSP-311e8	FEN1	AC004770	3.30	0.18						
Rad2	RAD2	NM_004111	4.07	0.55	Yes					
DNA repair										
<i>H.sapiens</i> DNA from chromosome 19p13.2	EKLF	AD000092	11.21	1.35						
Apurinic/apyrimidinic endonuclease-like 2 protein	APEXL2	AJ011311	4.86	1.25						+
X-ray repair, defective repair in CH cells 3	XRCC3	AF035586	3.00	0.32						
RAD51-interacting protein	PIR51	AF006259	3.02	0.20						
High-mobility group, chromosomal protein 2	HMG2	X62534	2.74	0.22	Yes		Yes			+
Bloom syndrome	BLM	U39817	2.20	0.22	Yes					+
RAD51 (<i>S.cerevisiae</i>) homolog C	RAD51C	AF029669	2.15	0.20			Yes		Yes	
Nudix-type motif 1	NUDT1	D16581	2.26	0.13						+
Xq28, 2000 bp sequence contig open reading frame (ORF)	HSXQ28ORF	X99270	2.08	0.13						+
Uracil-DNA glycosylase	UNG	Y09008	2.11	0.20				Yes	Yes	+
<i>H.sapiens</i> DNA from chromosome 19p13.2	EKLF	AD000092	1.94	0.21						
RuvB (<i>E.coli</i> homolog)-like 2	RUVBL2	AB024301	1.82	0.11						
Damage-specific DNA-binding protein 2 (48 kDa)	DDB2	U18300	1.74	0.13						+
Ubiquitin-conjugating enzyme E2N	UBE2N	D83004	1.80	0.09						+
RecQ protein-like (DNA helicase Q1-like)	RECQL	D37984	1.88	0.19						
NAD ⁺ ; poly (ADP-ribose) polymerase	ADPRT	J03473	1.61	0.10						+
RAD1 (<i>S.pombe</i>) homolog	RAD1	AF084513	1.84	0.18						
DNA (cytosine-5-)-methyltransferase 1	DNMT1	X63692	1.60	0.06				Yes		
Mitosis										
Kinesin-like 4	KNSL4	AB017430	18.92	2.02						+
Kinesin-like 5 (mitotic kinesin-like protein 1)	KNSL5	X67155	5.44	0.85					Yes	
Mitotic spindle coiled-coil related protein	DEEPEST	AF063308	4.68	0.26						
MAD2 (mitotic arrest deficient, yeast, homolog)-like 1	MAD2L1	AJ000186	4.16	0.95						+
<i>H.sapiens</i> lamin B1 gene, exon 11	lamin B1	L37747	4.68	0.38				Yes	Yes	
ZW10 interactor	ZWINT	AF067656	3.64	0.24						+
Budding uninhibited by benzimidazoles 1, beta	BUB1B	AF053306	3.48	0.41			Yes	Yes		
Centromere protein E (312 kDa)	CENPE	Z15005	3.76	0.41						
Kinesin-like 1	KNSL1	U37426	3.73	0.31				Yes		+
Chromosome-associated polypeptide C	CAP-C	AB019987	3.18	0.43						+
Chromosome-associated protein E (SMC family)	CAP-E	AF092563	3.56	0.52						+
Extra spindle poles, <i>S.cerevisiae</i> , homolog of	KIAA0165	D79987	2.67	0.21						+
Centromere protein A (17 kDa)	CENPA	U14518	2.85	0.10						
KIAA0042 gene product	KIAA0042	D26361	2.51	0.16						
Post-meiotic segregation increased 2-like 6	PMS2L6	AI341574	2.62	0.25						
Kinesin-like 6 (mitotic kinesin)	KNSL6	U63743	2.44	0.12						+
Chromosome 20 (ORF) 1	C20ORF1	AB024704	2.66	0.07						+
Kinesin-like 2	KNSL2	D14678	2.62	0.24				Yes		+
NIMA (never in mitosis gene a)-related kinase 2	NEK2	Z29066	2.67	0.22						
M-phase phosphoprotein 1	MPHOSPH1	L16782	2.25	0.13						
Tubulin, gamma 1	TUBG1	M61764	2.18	0.09						+
Centromere protein F (350/400 kDa, mitotin)	CENPF	U30872	2.05	0.18						+
Nucleolar phosphoprotein p130	P130	D21262	1.83	0.13						+
Chromosome segregation 1 (yeast homolog)-like	CSE1L	AF053641	1.76	0.07						+
Sjogren's syndrome/scleroderma autoantigen 1	SSSCA1	AB001740	1.70	0.08						
Chromosome condensation-related protein 1	KIAA0159	D63880	1.86	0.22						
Highly expressed in cancer, leucine heptad repeats	HEC	AF017790	4.95	0.32			Yes			+
MAD2 (mitotic arrest deficient, yeast, homolog)-like 1	MAD2L1	U65410	5.20	0.90						+
Structural maintenance of chromosomes 1-like 1	SMC1L1	D80000	1.72	0.14						+
Signal transduction										
Mitogen-activated protein kinase kinase kinase 14	MAP3K14	Y10256	4.41	0.92						
Transforming growth factor, beta receptor III	TGFBR3	L07594	3.22	0.46						
Transmembrane 4 superfamily member 1	TM4SF1	AI445461	3.25	0.19						
Mitogen-activated protein kinase kinase 3	MAP2K3	L36719	2.64	0.29						

Table 1. Continued

Gene description	Primary name	Accession no.	Mean FC	SD	Reference					E2F site
					(19)	(16)	(17)	(18)	(26)	
Low-density lipoprotein receptor gene, exon 18	LDLR	L00352	2.69	0.11						
Protein phosphatase 2A, regulatory subunit B'	PPP2R4	X73478	2.25	0.18						
Mitogen-activated protein kinase kinase 3	MAP2K3	D87116	2.33	0.25						
Protein tyrosine phosphatase, non-receptor type 1	PTPN1	M31724	2.01	0.22						
Phosphoglycerate kinase {alternatively spliced}	PGK	S81916	1.99	0.32						
Citron (rho-interacting, serine/threonine kinase 21)	CIT	AB023166	2.51	0.37						
Interleukin enhancer binding factor 1	ILF1	U58198	1.96	0.18						+
Protein kinase (cAMP-dependent) inhibitor alpha	PKIA	S76965	2.11	0.10						
G-protein-coupled receptor 19	GPR19	U64871	1.83	0.08						
Protein phosphatase 1G, gamma isoform	PPM1G	Y13936	1.81	0.10						
SFRS protein kinase 1	SRPK1	U09564	1.65	0.13						+
Protein phosphatase 2, reg. subunit B, delta isoform	PPP2R5D	L76702	1.58	0.05						
Tyrosine Kinase, receptor Axl, Alt. Splice 2	AXL	NM_001699	1.83	0.18						
Transcription										
c-myc binding protein	MYCBP	D50692	3.47	0.43						
v-myb homolog-like 1	MYBL1	X66087	3.03	0.36						
Thyroid hormone receptor interactor 13	TRIP13	U96131	3.09	0.12					Yes	
c-myc binding protein	MYCBP	AB007191	2.05	0.10						
TATA box binding protein (TBP)-associated factor	TAF2N	U51334	1.83	0.13						
Small nuclear RNA activating complex, polypeptide 1	SNAPC1	U44754	2.07	0.22						+
Putative DNA-binding protein	M96	AJ010014	1.83	0.09						+
Regulatory factor X, 5	RFX5	AL050135	1.77	0.11						
NF- κ B2 light polypeptide gene enhancer 2	NFKB2	X61498	1.77	0.14						
Polymerase (RNA) II (DNA-directed) polypeptide D	POLR2D	U89387	1.87	0.20						
NF- κ B inhibitor, epsilon	NFKBIE	U91616	1.66	0.10						
Forkhead box M1	FOXM1	U74612	3.82	0.26						+
Interleukin enhancer binding factor 1	ILF1	U58198	1.96	0.18						+
Associated with cancer										
Antigen identified by monoclonal antibody Ki-67	MKI67	X65550	7.32	2.11			Yes		Yes	+
Transmembrane 4 superfamily member 1	TM4SF1	M90657	3.93	0.24						
BRCA1-associated RING domain 1	BARD1	U76638	2.82	0.18	Yes					
Neurofibromin 2 (bilateral acoustic neuroma)	NF2	L11353	6.24	1.18						
RAB5C, member RAS oncogene family	RAB5C	U18420	4.50	1.02						
Ras-like protein Tc21	TC21	NM_012250	2.37	0.20						
Oncogene Aml1-Evi-1, fusion activated	Aml1-Evi-1		2.01	0.13						
Prostate tumor overexpressed gene 1	PTOV1	U79287	1.79	0.18						+
Mut homolog 2 (colon cancer, non-polyposis type 1)	MSH2	U03911	1.82	0.13				Yes		+
Non-metastatic cells 1, protein (NM23A)	NME1	AL038662	1.96	0.19						
Non-metastatic cells 1, protein (NM23A)	NME1	X73066	2.00	0.19						
Ras-GTPase-activating protein	G3BP	U32519	1.91	0.21						+
ras homolog gene family, member E	ARHE	S82240	1.76	0.14						
Human fibroblast growth factor-5 (FGF-5) mRNA	FGF5	M37825	5.16	0.34						
Inhibitor of DNA binding 1	ID1	X77956	4.04	0.20						
Cysteine and glycine-rich protein 2	CSRP2	U57646	2.66	0.20						
Nuclear RNA helicase	DDXL	U90426	2.19	0.17						
FGFR1 oncogene partner	FOP	Y18046	2.01	0.09						+
pim-2 oncogene	PIM2	U77735	1.89	0.10						

up-regulated 3.1-fold, while the transcriptional regulator ATRX was down-regulated 2.2-fold relative to control.

Mueller *et al.* (16) have reported that E2Fs induce the differentiation and development pathways, in particular, by upregulation of TGF β signaling genes. In our system, we did not observe any effect on these pathways (Figure 3). While the functional classification certainly affects the conclusion as to which pathways are affected (we used GO while Mueller *et al.* used GeneCards), in this case the low *Z*-score for the Cell Differentiation node ($Z = -0.7$) suggests that these processes are not affected in our experimental system.

It is likely that synchronization of cells prior to Rb knockdown would result in a stronger signal for the Rb knockdown signature (in the current system, the signal is diluted by those cells in the baseline experiment that are undergoing normal G₁/S transition). However our preliminary experiments

have shown that synchronization methods, such as serum starvation, cause additional changes in gene expression, thus complicating the interpretation of the treatment-specific changes (data not shown).

Identification of putative targets of the CDK4/6-pRb-E2F pathway

As the first step in identifying targets of the CDK4/6-pRb-E2F pathway, we selected genes up-regulated ≥ 1.5 -fold (P -value ≤ 0.05) from the Rb1 knockdown signature. This procedure generated a list of 469 genes (Supplementary Table 3), approximately half of which fall into the functional categories of cell cycle control, mitosis, DNA replication, DNA repair and signal transduction. We calculated the average fold changes and standard deviations for these genes

across all 10 experiments (5 siRNAs \times 2 replicates). Table 1 lists the genes falling into the aforementioned categories, along with the average fold changes and standard deviations. The low values of standard deviations indicate that the genes were similarly regulated by 5 different siRNAs in 10 independent experiments, which supports their association with the *Rb1* knockdown.

Our experiments produced a list of putative E2F targets. However, the fact that our genes are induced upon *Rb1* knockdown or the fact that some of them were induced upon E2F overexpression does not necessarily establish them as direct targets of the CDK4/6-pRb-E2F pathway. To further triage our list of putative targets, we analyzed the promoter sequences of these genes to identify E2F binding motifs.

Several reports have been recently published on putative E2F targets (16–19). In a recent study, Vernell *et al.* (19) have performed a cross-comparison of the gene list generated by overexpression of *E2F* with a gene list obtained by expression of a phosphorylation-site mutant of *Rb1* or *p16*. The authors have identified 74 genes that are up-regulated upon overexpression of *E2F* and down-regulated upon expression of *Rb1* and *p16*. Many of these genes contained sequences enriched in the *E2F*-binding motif and therefore are good candidates for CDK4/6-pRb-E2F pathway targets. However, other reports (17,18,31,33) pointed out under-representation of cell cycle and checkpoint regulators in the target lists of Vernell *et al.*

Ishida *et al.* (17) have synchronized a mouse embryonic fibroblast (MEF) cell line at G₁/S, overexpressed *E2F-1*, *E2F-2* and *E2F-3* genes in these cells using an adenoviral vector, and performed microarray analysis. The study yielded a list of 65 putative targets, which have not been subjected to promoter analysis. Polager *et al.* (18) generated rat cell lines containing inducible *E2F-1* and *E2F-3* and generated gene expression profiles associated with *E2F* overexpression. The list of genes up-regulated upon *E2F-1* and *E2F-3* expression contained 72 genes and ESTs, many of which were associated with the S and M phases of the cell cycle. Black *et al.* (26) have generated expression profiles for serum-starved mouse embryonic fibroblasts null for *Rb1*, *p107* and *p130*, and applied the statistical tools developed for expression-based tumour classification. The results indicated clear differences in the expression patterns.

We compared the lists of genes reported in these studies with our set of putative targets. The results summarized in Table 1 reveal that only 53 out of 178 (30%) genes identified in our experiments have previously been suggested as putative targets of the CDK4/6-pRb-E2F pathway. Furthermore, our analysis reveals a small degree of overlap between the datasets obtained in the previous studies (16–19,26). This could be attributed to the fact that the previous studies involved different experimental systems, namely, ectopic overexpression of *E2Fs* or introduction of a mutant pRb. Our approach using a transient *Rb1* knockdown mimics the normal progression of the cells cycle, when *Rb1* is inactivated by phosphorylation at the G₁/S transition. The variance in the published results can also be due to the fact that different timepoints and different organisms were used. Another possible explanation is that the *E2F* overexpression studies utilized *E2F1* and *E2F3* constructs, while *Rb1* is known to bind to *E2Fs* 1 through 4 and also interact with chromatin-remodeling complexes [for reviews, see (11–13)].

In Table 1, the putative CDK4/6-pRb-E2F pathway targets are classified into functional categories. It can be seen that majority of the genes previously implicated in the pathway are in the categories of DNA biosynthesis (21 out of 46), cell cycle (17 out of 36) and DNA repair (5 out of 18). The novel genes in the cell cycle category are *CDC25C*, *CDC28*, *Chk1*, *cyclins C*, *D3* and *F*, *STK12*, *STK15* (*Aurora 2 kinase*), *TTK protein kinase*, *CDKN3*, *ASK*, *GSPT1*, *SNK* and *RASSF1*. Among these genes, only *STK15*, *TTK*, *GSPT1*, *CDC28*, *E2F2* and *Chk1* have E2F-binding sites. Thus, they are likely to be direct targets of the CDK4/6-pRb-E2F pathway, while *cyclins C*, *D3* and *F*, and *CDC25C*, *CDC28*, *STK12*, *RASSF1*, *SNK*, *CDKN3* and *GOS2* may be induced through different mechanisms. It is known that *Rb1* can regulate transcription through chromatin modification mechanisms by forming complexes with HDACs [reviewed in (11,34)].

The *STK15/STK6* (*Aurora A kinase*) is known to be induced at the G₂/M transition and during mitosis, and to be involved in cell cycle checkpoint and chromosome segregation. However, it has not been previously implicated in the CDK4/6-pRb-E2F pathway. It has previously been shown (35) that the E2 ubiquitin-conjugating enzyme (*UBE2N*) binds to *STK15/STK6* in human cells resulting in co-localization of the two enzymes in the centrosomes during mitosis. In our experiments, both *STK15/STK6* and *UBE2N* were concurrently induced (Table 1), which is consistent with their involvement in the same mitotic complex. *STK15/STK6* has also been shown (36) to bind protein phosphatase type 1, another gene induced in our experiments, in a cell-cycle-dependent manner. Thus, the associations between *STK15/STK6* and other members of the *Rb1* knockdown signature support the finding that this enzyme is a novel target of the CDK4/6-pRb-E2F pathway.

Chk1 is another gene implicated in this study as a potential direct target of the CDK4/6-pRb-E2F pathway. This gene has previously been reported to have E2F1 functional sites (31), but has not been identified in microarray screens (16–19) as a target of the pathway. Our finding is consistent with the involvement of *Rb1* in the DNA damage response pathway (discussed in the previous section).

The Transcription and Signal Transduction categories in Table 1 are relatively rich in genes that have not been previously associated with the *Rb1* pathway. One of the most interesting findings here is the possibility that the forkhead transcription factor is a direct target of the CDK4/6-pRb-E2F pathway. The *FOXM1* gene is induced 3.8-fold upon *Rb1* knockdown, and it has an E2F site. Wang *et al.* (37) have shown that the *FOXMI*B transcription factor regulates expression of cell cycle proteins essential for hepatocyte entry into DNA replication and mitosis. It is possible that the forkhead transcription factor may be the link that connects the CDK4/6-pRb-E2F pathway with the multiple mitotic targets that are not directly induced by E2Fs.

The *MYCBP* (*AMY-1*) gene (2.1-fold induction; no E2F site) encodes a protein that binds to the N-terminal region of *MYC* and stimulates the activation of E-box-dependent transcription by *MYC* (38). This target may serve as a link between the CDK4/6-pRb-E2F pathway and *MYC*-mediated proliferation control, which includes induction of *CDC25A*, another indirect target of the CDK4/6-pRb-E2F pathway identified in our analysis.

CONCLUSIONS

We applied siRNA-mediated gene silencing coupled with microarray screening and systematic pathway analysis to obtain insights into the pathways controlled by the target gene. This approach represents a promising strategy in functional genomics, as it allows the researcher to determine the role of the target gene in intracellular pathways. In the future, this approach may be used to create a database of gene expression signatures for various perturbations, such as siRNA-mediated gene knockdowns and treatments with small-molecule inhibitors. This database would then be used as a reference table to analyze new profiles obtained for novel inhibitors, thus providing value in drug target identification and candidate compound selection. Classification based on expression signatures has been applied to cancer and resulted in new drug targets (39–41).

By applying Gene Ontology-based pathway analysis tools, we identified the effects of *Rb1* knockdown on cellular pathways. Consistent with previous microarray studies of E2F overexpression, *Rb1* knockdown affected G₁/S and G₂/M transitions of the cell cycle, DNA replication and repair, mitosis, and apoptosis, indicating that siRNA-mediated transient elimination of Rb1 mimics the control of cell cycle through Rb1 dissociation from E2F. Additionally, we observed significant effects on the processes of DNA damage response and epigenetic regulation of gene expression. Our data suggest that *Rb1* is involved in the control of the DNA damage response in addition to the regulation of DNA replication and concurrent DNA repair. Analysis of E2F-binding sites is suggested as a method to distinguish between putative direct targets and genes induced through other mechanisms. Another promising approach is to obtain a time course of expression changes and distinguish between direct targets and secondary effects based on the timing of gene expression changes in response to the knockdown of the target.

SUPPLEMENTARY MATERIAL

Supplementary Material is available at NAR Online.

ACKNOWLEDGEMENTS

We thank Aparna Sarthy, Xiaoli Huang and Leigh Frost for expert technical assistance, Joel Levenson and Mark Schurdak for helpful and stimulating discussions, and Haiying Zhang and Yan Luo for critical reading of the manuscript.

REFERENCES

- Elbashir, S.M., Lendeckel, W. and Tuschl, T. (2001) RNA interference is mediated by 21- and 22-nucleotide RNAs. *Genes Dev.*, **15**, 188–200.
- Elbashir, S.M., Harborth, J., Lendeckel, W., Yalcin, A., Weber, K. and Tuschl, T. (2001) Duplexes of 21-nucleotide RNAs mediate RNA interference in cultured mammalian cells. *Nature*, **411**, 494–498.
- Zamore, P.D. (2001) RNA interference: listening to the sound of silence. *Nature Struct. Biol.*, **8**, 746–750.
- Sharp, P.A. (2001) RNA interference—2001. *Genes Dev.*, **15**, 485–490.
- McManus, M.T. and Sharp, P.A. (2002) Gene silencing in mammals by small interfering RNAs. *Nature Rev. Genet.*, **3**, 737–747.
- Bernstein, E., Denli, A.M. and Hannon, G.J. (2001) The rest is silence. *RNA*, **7**, 1509–1521.
- Dykxhoorn, D.M., Novina, C.D. and Sharp, P.A. (2003) Killing the messenger: short RNAs that silence gene expression. *Nature Rev. Mol. Cell. Biol.*, **4**, 457–467.
- Wall, N.R. and Shi, Y. (2003) Small RNA: can RNA interference be exploited for therapy? *Lancet*, **362**, 1401–1403.
- Semizarov, D., Frost, L., Sarthy, A., Kroeger, P., Halbert, D.N. and Fesik, S.W. (2003) Specificity of short interfering RNA determined through gene expression signatures. *Proc. Natl Acad. Sci. USA*, **100**, 6347–6352.
- Ashburner, M., Ball, C.A., Blake, J.A., Botstein, D., Butler, H., Cherry, J.M., Davis, A.P., Dolinski, K., Dwight, S.S., Eppig, J.T. et al. (2000) Gene ontology: tool for the unification of biology. The Gene Ontology Consortium. *Nature Genet.*, **25**, 25–29.
- Classon, M. and Harlow, E. (2002) The retinoblastoma tumour suppressor in development and cancer. *Nature Rev. Cancer*, **2**, 910–917.
- Kaelin, W.G., Jr (1999) Functions of the retinoblastoma protein. *Bioessays*, **21**, 950–958.
- Dyson, N. (1998) The regulation of E2F by pRB-family proteins. *Genes Dev.*, **12**, 2245–2262.
- Qin, X.Q., Livingston, D.M., Ewen, M., Sellers, W.R., Arany, Z. and Kaelin, W.G., Jr (1995) The transcription factor E2F-1 is a downstream target of RB action. *Mol. Cell. Biol.*, **15**, 742–755.
- Nevins, J.R. (1992) E2F: a link between the Rb tumor suppressor protein and viral oncoproteins. *Science*, **258**, 424–429.
- Muller, H., Bracken, A.P., Vernell, R., Moroni, M.C., Christians, F., Grassilli, E., Prosperini, E., Vigo, E., Oliner, J.D. and Helin, K. (2001) E2Fs regulate the expression of genes involved in differentiation, development, proliferation, and apoptosis. *Genes Dev.*, **15**, 267–285.
- Ishida, S., Huang, E., Zuzan, H., Spang, R., Leone, G., West, M. and Nevins, J.R. (2001) Role for E2F in control of both DNA replication and mitotic functions as revealed from DNA microarray analysis. *Mol. Cell. Biol.*, **21**, 4684–4699.
- Polager, S., Kalma, Y., Berkovich, E. and Ginsberg, D. (2002) E2Fs up-regulate expression of genes involved in DNA replication, DNA repair and mitosis. *Oncogene*, **21**, 437–446.
- Vernell, R., Helin, K. and Muller, H. (2003) Identification of target genes of the p16INK4A-pRB-E2F pathway. *J. Biol. Chem.*, **278**, 46124–46137.
- Reynolds, A., Leake, D., Boese, Q., Scaringe, S., Marshall, W.S. and Khvorov, A. (2004) Rational siRNA design for RNA interference. *Nat. Biotechnol.*, **22**, 326–330.
- Khvorov, A., Reynolds, A. and Jayasena, S.D. (2003) Functional siRNAs and miRNAs exhibit strand bias. *Cell*, **115**, 209–216.
- Dahlquist, K.D., Salomonis, N., Vranizan, K., Lawlor, S.C. and Conklin, B.R. (2002) GenMAPP, a new tool for viewing and analyzing microarray data on biological pathways. *Nature Genet.*, **31**, 19–20.
- Doniger, S.W., Salomonis, N., Dahlquist, K.D., Vranizan, K., Lawlor, S.C. and Conklin, B.R. (2003) MAPPFinder: using Gene Ontology and GenMAPP to create a global gene-expression profile from microarray data. *Genome Biol.*, **4**, R7.
- Kel, A.E., Kel-Margoulis, O.V., Farnham, P.J., Bartley, S.M., Wingender, E. and Zhang, M.Q. (2001) Computer-assisted identification of cell cycle-related genes: new targets for E2F transcription factors. *J. Mol. Biol.*, **309**, 99–120.
- Ohtani, K., Iwanaga, R., Nakamura, M., Ikeda, M., Yabuta, N., Tsuruga, H. and Nojima, H. (1999) Cell growth-regulated expression of mammalian MCM5 and MCM6 genes mediated by the transcription factor E2F. *Oncogene*, **18**, 2299–2309.
- Black, E.P., Huang, E., Dressman, H., Rempel, R., Laakso, N., Asa, S.L., Ishida, S., West, M. and Nevins, J.R. (2003) Distinct gene expression phenotypes of cells lacking Rb and Rb family members. *Cancer Res.*, **63**, 3716–3723.
- Helin, K. (1998) Regulation of cell proliferation by the E2F transcription factors. *Curr. Opin. Genet. Dev.*, **8**, 28–35.
- Blattner, C., Sparks, A. and Lane, D. (1999) Transcription factor E2F-1 is upregulated in response to DNA damage in a manner analogous to that of p53. *Mol. Cell. Biol.*, **19**, 3704–3713.
- O'Connor, D.J. and Lu, X. (2000) Stress signals induce transcriptionally inactive E2F-1 independently of p53 and Rb. *Oncogene*, **19**, 2369–2376.
- Hofferer, M., Wirbelauer, C., Humar, B. and Krek, W. (1999) Increased levels of E2F-1-dependent DNA binding activity after UV- or gamma-irradiation. *Nucleic Acids Res.*, **27**, 491–495.

31. Ren,B., Cam,H., Takahashi,Y., Volkert,T., Terragni,J., Young,R.A. and Dynlacht,B.D. (2002) E2F integrates cell cycle progression with DNA repair, replication, and G₂/M checkpoints. *Genes Dev.*, **16**, 245–256.
32. Sage,J., Mulligan,G.J., Attardi,L.D., Miller,A., Chen,S., Williams,B., Theodorou,E. and Jacks,T. (2000) Targeted disruption of the three Rb-related genes leads to loss of G₁ control and immortalization. *Genes Dev.*, **14**, 3037–3050.
33. Weinmann,A.S., Yan,P.S., Oberley,M.J., Huang,T.H. and Farnham,P.J. (2002) Isolating human transcription factor targets by coupling chromatin immunoprecipitation and CpG island microarray analysis. *Genes Dev.*, **16**, 235–244.
34. Harbour,J.W. and Dean,D.C. (2000) The Rb/E2F pathway: expanding roles and emerging paradigms. *Genes Dev.*, **14**, 2393–2409.
35. Ewart-Toland,A., Briassouli,P., de Koning,J.P., Mao,J.H., Yuan,J., Chan,F., MacCarthy-Morrogh,L., Ponder,B.A., Nagase,H., Burn,J. *et al.* (2003) Identification of Stk6/STK15 as a candidate low-penetrance tumor-susceptibility gene in mouse and human. *Nature Genet.*, **34**, 403–412.
36. Katayama,H., Zhou,H., Li,Q., Tatsuka,M. and Sen,S. (2001) Interaction and feedback regulation between STK15/BTAK/Aurora-A kinase and protein phosphatase 1 through mitotic cell division cycle. *J. Biol. Chem.*, **276**, 46219–46224.
37. Wang,X., Kiyokawa,H., Dennewitz,M.B. and Costa,R.H. (2002) The Forkhead Box m1b transcription factor is essential for hepatocyte DNA replication and mitosis during mouse liver regeneration. *Proc. Natl Acad. Sci. USA*, **99**, 16881–16886.
38. Taira,T., Maeda,J., Onishi,T., Kitaura,H., Yoshida,S., Kato,H., Ikeda,M., Tamai,K., Iguchi-Ariga,S.M. and Ariga,H. (1998) AMY-1, a novel C-MYC binding protein that stimulates transcription activity of C-MYC. *Genes Cells*, **3**, 549–565.
39. Ramaswamy,S., Tamayo,P., Rifkin,R., Mukherjee,S., Yeang,C.H., Angelo,M., Ladd,C., Reich,M., Latulippe,E., Mesirov,J.P. *et al.* (2001) Multiclass cancer diagnosis using tumor gene expression signatures. *Proc. Natl Acad. Sci. USA*, **98**, 15149–15154.
40. van't Veer,L.J., Dai,H., van de Vijver,M.J., He,Y.D., Hart,A.A., Mao,M., Peterse,H.L., van der Kooy,K., Marton,M.J., Witteveen,A.T. *et al.* (2002) Gene expression profiling predicts clinical outcome of breast cancer. *Nature*, **415**, 530–536.
41. Bittner,M., Meltzer,P., Chen,Y., Jiang,Y., Seftor,E., Hendrix,M., Radmacher,M., Simon,R., Yakhini,Z., Ben-Dor,A. *et al.* (2000) Molecular classification of cutaneous malignant melanoma by gene expression profiling. *Nature*, **406**, 536–540.